frontiers | Frontiers in Earth Science

TYPE Original Research
PUBLISHED 15 August 2023
DOI 10.3389/feart.2023.1205849

OPEN ACCESS

EDITED BY
Sung Keun Lee,
Seoul National University, Republic of Korea

REVIEWED BY
Qiang Guo,
China University of Mining and Technology, China
Ali Abedini,
Urmia University, Iran
Rui Liu,
Southwest Petroleum University, China

*CORRESPONDENCE
Yansheng Shan,
danyansheng@mail.cgs.gov.cn
Leilei Yang,
yangleilei@cup.edu.cn

†These authors have contributed equally to this work and share first authorship

RECEIVED 17 April 2023
ACCEPTED 14 July 2023
PUBLISHED 15 August 2023

CITATION
Yang L, Lu L, Li X, Shan Y, Mo C, Sun M, Hu J, Liu W, Liang B and Xu J (2023), Clay mineral transformation mechanism modelling of shale reservoir in Da'anzhai Member, Sichuan Basin, Southern China. *Front. Earth Sci.* 11:1205849. doi: 10.3389/feart.2023.1205849

Clay mineral transformation mechanism modelling of shale reservoir in Da'anzhai Member, Sichuan Basin, Southern China

Leilei Yang[1,2,3†]*, Longfei Lu[1,2,3†], Xiaowei Li[3], Yansheng Shan[4]*, Chenchen Mo[3], Meng Sun[5], Jing Hu[3], Weibin Liu[4], Baoxing Liang[6] and Jin Xu[1,2]

[1]State Key Laboratory of Shale Oil and Gas Enrichment Mechanisms and Effective Development, Beijing, China, [2]SINOPEC Key Laboratory of Petroleum Accumulation Mechanisms, Wuxi, China, [3]State Key Laboratory of Petroleum Resource and Prospecting, China University of Petroleum (Beijing), Beijing, China, [4]Oil and Gas Survey, China Geological Survey, Beijing, China, [5]Exploration and Development Research Institute of Huabei Oilfield Company, China National Petroleum Corporation, Renqiu, China, [6]Experimental Testing Research Institute, Xinjiang Oilfield Company, CNPC, Karamay, Xinjiang, China

Shale reservoirs often undergo intense clay mineral transformation, which plays a crucial role in the formation and evolution of pores. The reservoir lithofacies types of Da'anzhai Member in the Sichuan Basin are complex, the heterogeneity is strong, and the transformation mechanism of clay minerals is unclear, limiting the understanding of reservoir diagenesis and reservoir formation mechanism. In this study, we selected the typical shale reservoir in the Da'anzhai Member of the eastern Sichuan Basin and innovatively introduced the multiphase fluid-chemical-thermal multi-field coupled numerical simulation technique to focus on the dissolution, precipitation and transformation laws of diagenetic minerals in the shale reservoir. We calculated the transformation of diagenetic minerals and their physical response under different temperatures, pressure and fluid conditions and identified the main controlling factors of mineral transformation in shale reservoirs in the study area. The results show that the transformation of smectite to illite in the Da'anzhai Member is a complex physicochemical process influenced by various factors such as temperature, pressure, fluid, and lithology. The increase in temperature can promote illitization until the critical temperature of 110°C–115°C, below which the conversion rate of smectite to illite increases as the temperature increases. However, when it is higher than the critical temperature, the degree of illitization decreases. In specific K-rich fluids, organic acids significantly affect the conversion of clay minerals in the Da'anzhai Member of the formation. The acidic fluid promotes the dissolution of minerals such as K-feldspar and releases K^+, thus provides the material basis for illitization. The research results provide theoretical support for the diagenetic and formation mechanism of the shale reservoir in the Da'anzhai Member of the Sichuan Basin and even for the efficient exploration and development of shale gas.

KEYWORDS

shale reservoirs, clay minerals, K-rich fluid, porosity, main controlling factors

1 Introduction

Unconventional oil and gas resources have great potential as strategic replacements for current storage and production, they are expected to change the global energy structure, allowing China to achieve its "double carbon" goal through energy transformation (Gracceva and Zeniewski, 2013; Shuen et al., 2014; Kamiński et al., 2017). Many wells in the Yuanba area of northeastern Sichuan have obtained medium to high-yield industrial gas flow in the Da'anzhai member of the Jurassic Ziliujing Formation, which proves the good continental shale gas accumulation conditions and exploration potential in northeastern Sichuan (Jiao et al., 2020; Zou et al., 2020).

The key to oil and gas exploration lies in reservoir quality evaluation, and clarifying the diagenetic development mechanism of reservoirs is the premise of reservoir quality evaluation. As a source-reservoir integrated resource, diagenesis controls the mineral composition, microstructure and reservoir properties and significantly influences the generation and migration of oil and gas (Bernard et al., 2012; Baruch et al., 2015; Ma et al., 2017; Shangbin et al., 2017; Zou et al., 2022). The mineral types of shale reservoirs are complex, and a series of organic-inorganic interactions occur during diagenesis, resulting in changes in ion concentration, element migration, and mineral transformation, thus changing the reservoir's physical conditions (Baruch et al., 2015; Borjigin et al., 2021).

The reservoir lithofacies types of Da'anzhai Member in the Sichuan Basin are complex, and the heterogeneity is strong, clay shale and mixed shale are the most developed (Sun et al., 2020; Liu et al., 2021; Yang et al., 2022; Jiang et al., 2023a; Xiong et al., 2023). The mineral content varies little in layers but significantly in regions and is dominated by calcite-based carbonate, clay minerals and quartz, the shale reservoir in the Da'anzhai member underwent an intense transformation of clay minerals, which is crucial to forming and evolving pores (Zhu et al., 2022). However, mineral transformation is controlled by several factors, such as temperature, fluid, and chemical action, the intricate relationships limit the understanding of mineral transformation in the Da'anzhai member, which hinders the study of the reservoir diagenesis and formation mechanism (Bjlykke, 1998; Zhang et al., 2010).

Based on this, this study selects a typical shale reservoir in the Da'anzhai member of the eastern Sichuan basin and innovatively introduces a multiphase fluid-chemical-thermal multi-field coupled numerical simulation technique to focus on the dissolution, precipitation and transformation of shale reservoir diagenetic minerals. Based on qualitative analysis, the transformation of diagenetic minerals and their physical properties response under different temperatures, pressure and fluid conditions are quantitatively calculated, and the main controlling factors of mineral transformation in shale reservoirs in the study area are identified, which provides theoretical support for the diagenesis and reservoir formation mechanism of shale reservoirs and even efficient exploration and development of shale gas.

2 Geological background

As shown in Figures 1A–C, the study area is located northeast of the Sichuan basin. The lithology of the continental shale strata system in northeastern Sichuan changes rapidly; the heterogeneity is strong, the lamina is developed, the single layer thickness of shale is thin, and the cumulative thickness is large (Sca et al., 2019). The Da'anzhai Member of the Ziliujing Formation has good hydrocarbon displays. The Da'anzhai Member sediments mainly develop shore lake, shallow lake and semi-deep lake subphase, and the high-quality shales are mainly distributed in the semi-deep lake subphase near the subsidence center of the lake basin (Tan et al., 2016; Yang et al., 2020; Xu et al., 2022).

The stratigraphic thickness of the Da'anzhai Member ranges from 70 to 138 m and can be divided from bottom to top into the third sub-Member (5–20 m), the second sub-Member (24–65 m) and the first sub-Member (40–63 m) (Zheng et al., 2013; Zhu et al., 2022). Due to the frequent changes in the lake level, the Da'anzhai Member has caused the interbedded deposition of shale and thin-bedded limestone and sandstone. Both the third sub-Member and the first sub-Member are thickly bedded limestone with thinly bedded shales, and the second sub-Member is shales with thinly bedded limestone (Li et al., 2020a).

The mineral composition of the Da'anzhai Member in northeastern Sichuan is mainly quartz, clay minerals and calcite, among which clay minerals and quartz are generally high, and the relative content is greater than 35%, the content of calcite minerals varies widely, with high content in limestone and local enrichment (Xu et al., 2019; Liu et al., 2020; Jiang et al., 2023b).

The reservoir of Da'anzhai member has the characteristics of ultra-low porosity and ultra-low permeability, which is a typical and highly heterogeneous unconventional tight reservoir (Liu, 2021; Liu et al., 2021; Yang et al., 2022; Jiang et al., 2023a). The reservoir space is divided into two types: pores and fractures; the pore types are organic matter pores, intergranular pores, intercrystalline pores, dissolution pores and micropores between clay minerals; the fractures include structural fractures, shale bedding fractures and diagenetic shrinkage fractures.

According to the analysis of burial history and thermal evolution history, two obvious uplifts occurred in Da 'anzhai, northeastern Sichuan. The first uplift occurred at 140 MPa, which is also the time of the first crude oil filling. The second uplift occurred at 25 Ma, which is the time of the second oil and gas filling (Xie et al., 2023). And the second oil and gas filling, so that the formation of a large number of pore water discharge, may also be the reason for the inhibition of illite.

There are many types and stages of diagenesis in Da'anzhai Member, including compaction, cementation, dissolution, metasomatism, recrystallization, the transformation of clay minerals and diagenetic evolution of organic matter (Sun et al., 2020; Zhu et al., 2022). Among them, compaction, metasomatism and recrystallization are the main destructive effects, and dissolution and fracture are the main constructive effects.

3 Numerical simulation

3.1 Simulation scheme

(1) To study the influence of single factors (temperature and pressure, fluid, and rock and ore) on the transformation of smectite and kaolinite to illite in the reservoir, 20 sets of models were set up, corresponding to different temperatures and

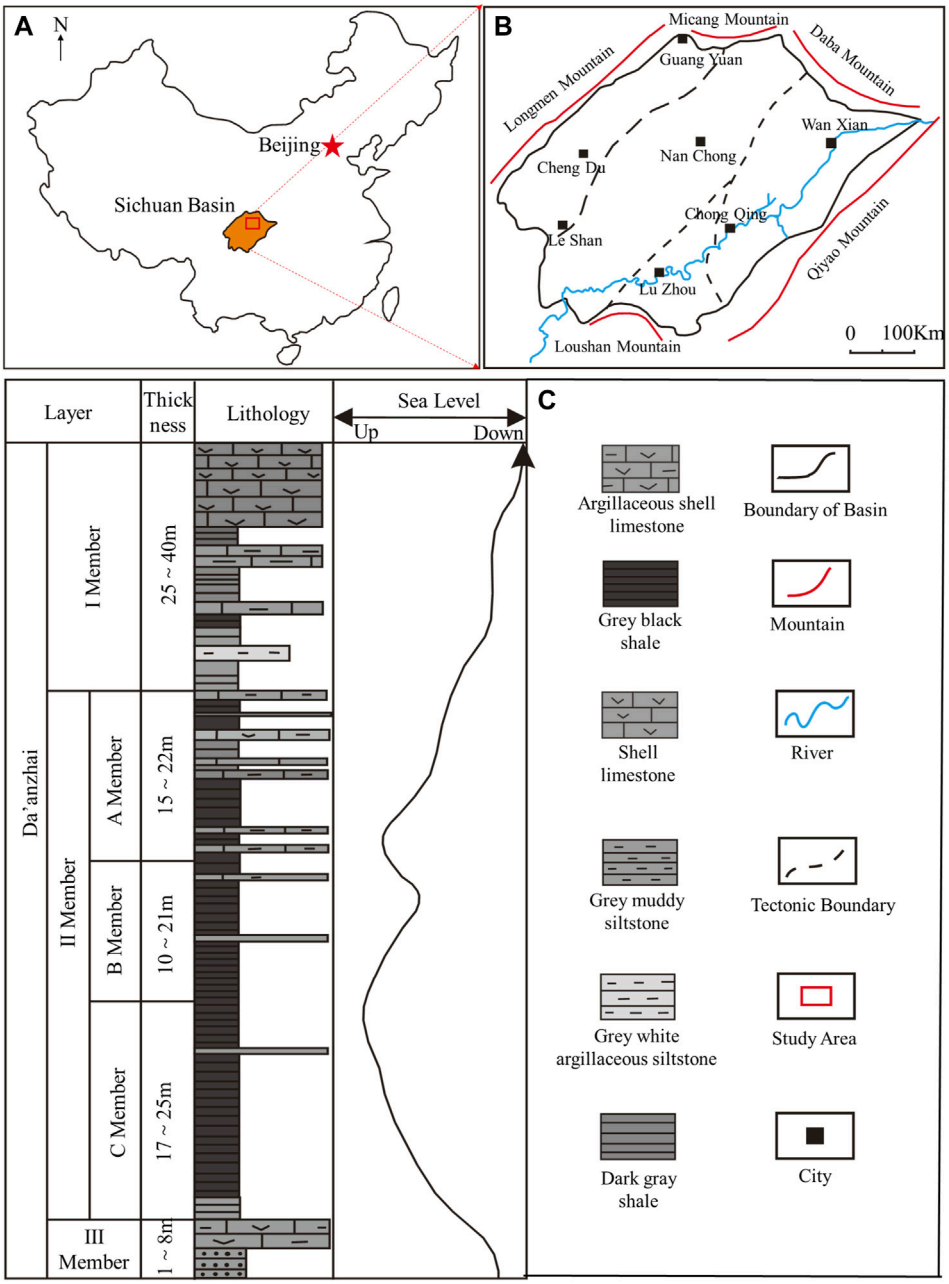

FIGURE 1
Comprehensive histogram of the tectonic unit and the Da'anzhai member in the Sichuan Basin (Kang et al., 2022).

pressure, fluid, and rock and ore conditions. Cases 1–8 correspond to different temperatures and pressure, 9–12 correspond to different fluids, 13–16 correspond to different smectite content, and 17–20 correspond to different illite content.

(2) In order to further study the influence of temperature, pressure, fluid, rock and mineral factors on the conversion of montmorillonite and kaolinite to illite in the reservoir. A two-dimensional heterogeneous model of the Member was established to study the actual influence of the interaction on the mineral evolution of the Da 'anzhai formation under comprehensive factors.

3.2 Model tool

Numerical simulation software TOUGHREACT was used. Geochemical reactions are introduced into the phase flow and heat flow software TOUGH2. TOUGHREACT considers the effects of mineral dissolution and precipitation on formation porosity and permeability and can be well applied to many geological problems (Xu et al., 2006; Yang et al., 2023).

The principle of TOUGHREACT is conservation of mass and conservation of energy. The coupling process of temperature field-hydraulic field-chemical field (T-H-C) can be divided into three relatively independent reaction processes: multiphase flow and heat

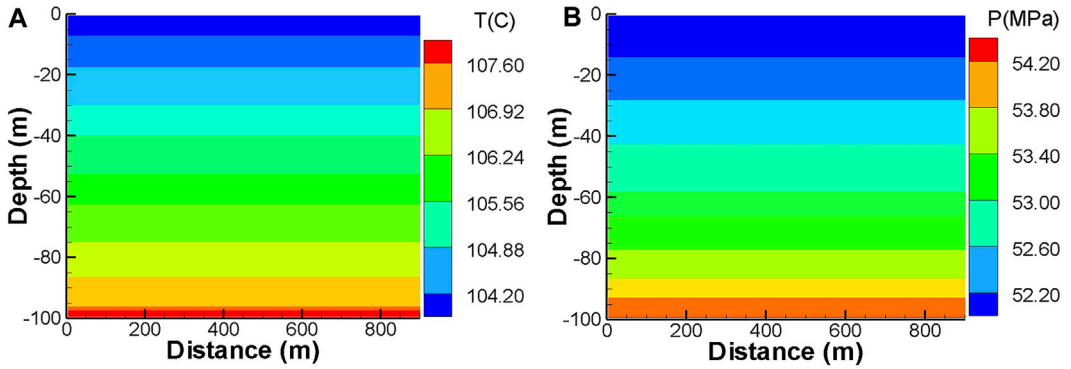

FIGURE 2
Initial temperature and pressure distribution diagram.

transfer, solute transport and chemical reaction. Based on the law of conservation of mass and energy, the three processes are described by Darcy's law, Fick's law and mass action law respectively, and the mathematical model of thermal-hydrodynamic-chemical is established. Variable saturated flow can be described by a complete set of multiphase flow conservation equations. For multiphase flow and heat transfer process, mainly includes four parts: 1) fluid flow in the liquid phase or gas phase driven by pressure, viscosity and gravity; 2) The interaction between the flow phase states represented by the characteristic curve (relative permeability and capillary pressure); 3) Convective conduction and advection conduction of heat; 4) Diffusion of water vapor and air. In the calculation of thermophysical and geochemical properties, the density, viscosity, thermodynamic and kinetic data of mineral-water-gas reactions of fluids (gas and liquid) are all calculated as functions of temperature. In both liquid and gas phases, convection and molecular diffusion during the migration of water phase ions and gas phase components are considered.

3.3 Numerical model

3.3.1 One-dimensional mechanistic model

We established a classic three-grid model with inflow on the left, outflow on the right, and simulated grids in the middle to monitor mineral content, ion concentration, and porosity changes.

3.3.2 Two-dimensional profile model

The actual burial depth of the Da'anzhai member is 3,800–4,100 m. To reconstruct the mineral transformation on the profile of the Da'anzhai member, we inferred that the burial depth of mineral transformation is 3,000–3,100 m according to the burial history and diagenetic evolution process. The vertical (Z) of the selected layer is 100 m, divided into 100 grids of 1 m each. The model has 1,000 m in the transverse direction (X) and is divided into 60 grids. The volume of the grid increases from left to right.

3.4 Initial conditions

3.4.1 Reservoir geological conditions

According to the measured data of the Da'anzhai Member in the study area, the continental fine-grained sedimentary rocks in the Da'anzhai Member belong to the pore-fracture reservoir with ultra-low porosity and low permeability. The maximum porosity of the Da'anzhai Member in Yuanba area is 6.8%, the minimum porosity is 2.1%, and the average porosity is 3.35%. The maximum permeability is $0.6/(10^{-3}\ \mu m^2)$, the minimum permeability is $0.008/(10^{-3}\ \mu m^2)$, and the average permeability is $0.08/(10^{-3}\ \mu m^2)$. In the one-dimensional model, the porosity and permeability are averaged. In the two-dimensional model, the initial formation properties were therefore inferred in order to reconstruct the mineral transformation process. The three sets of strata in the model, corresponding to porosity and permeability, are $10.5\%/0.9/(10^{-3}\ \mu m^2)$, $14.4\%/0.4/(10^{-3}\ \mu m^2)$, and $13.3\%/0.8/(10^{-3}\ \mu m^2)$, respectively.

The overpressure is generally developed in the shale reservoirs of the Da'anzhai member in the study area. The pressure coefficient is 1.30–2.07 MPa/100 m, the formation pressures range from 40 to 78 MPa, and the geothermal gradient is 2.28°C/100 m. In the one-dimensional model, the temperature and pressure of Case1-11 are 50°C/10.7 MPa, 60°C/18.4 MPa, 70°C/26.1 MPa, 80°C/33.8 MPa, 90°C/41.1 MPa, 104°C/52.5 MPa, 110°C/56 MPa, 115°C/58 MPa, 120°C/62 MPa, 125°C/63 MPa, and 132°C/65 MPa. The temperature and pressure of Case12-23 are consistent at 131.5°C and 65.0 MPa, respectively.

In the two-dimensional model, according to the temperature and pressure corresponding to the burial depth of 3,000–3,100 m, the temperature and pressure at the top and bottom of the model are 104.4°C/52.5 MPa and 106.7°C/54.25 MPa, respectively, and the distribution is shown in Figures 2A, B.

3.4.2 Water chemistry conditions

This simulation has four kinds of formation water and a K-rich fluid. Among them, the one-dimensional model contains one kind of formation water, and the two-dimensional model contains three kinds of lithology, corresponding to three kinds of formation water. The formation water compositions are all equilibrated from the actual water chemistry data, and the formation water is in equilibrium with the rock minerals.

The organic acid development in the Da'anzhai member of the study area and the dissolution of feldspar by organic acid make the reservoir a K-rich environment. Therefore, the concentration of K^+ is about three times that of formation water when the K-rich fluid is injected. The chemical composition and ion concentration of water are shown in Table 1.

TABLE 1 Water chemical composition and ion concentration.

Ion type	Stratigraphic water in 1-D model mol/kg H_2O	Stratigraphic water 1in 2-D model mol/kg H_2O	Stratigraphic water 2in 2-D model mol/kg H_2O	Stratigraphic water 3in 2-D model mol/kg H_2O	Rich K fluidin 2-D model mol/kg H_2O
Ca^{2+}	1.3049×10^{-4}	1.6614×10^{-6}	1.6837×10^{-6}	1.7176×10^{-6}	1.3049×10^{-4}
Mg^{2+}	1.0226×10^{-4}	5.3739×10^{-8}	1.1743×10^{-7}	5.1446×10^{-8}	1.0226×10^{-4}
K^{+}	1.3760×10^{-5}	1.4089×10^{-6}	1.1967×10^{-6}	1.5072×10^{-6}	4.1280×10^{-2}
Na^{+}	1.3155×10^{-2}	6.2579×10^{-3}	6.2556×10^{-3}	6.2522×10^{-3}	1.3155×10^{-2}
Cl^{-}	9.3142×10^{-3}	9.3300×10^{-3}	9.3266×10^{-3}	9.3215×10^{-3}	9.3142×10^{-3}
HCO_3^{-}	3.4547×10^{-6}	7.3922×10^{-4}	7.4795×10^{-4}	7.6108×10^{-4}	3.4547×10^{-6}
SO_4^{2-}	8.7765×10^{-5}	9.3364×10^{-5}	9.3318×10^{-5}	9.3268×10^{-5}	8.7765×10^{-5}
SiO_2 (aq)	8.4924×10^{-4}	8.4130×10^{-4}	8.4560×10^{-4}	8.4101×10^{-4}	8.4924×10^{-4}

TABLE 2 Mineral type and content.

Name	R1	R2	R3	R4	R5	R6	R7	R8	R9	R10	R11
Calcite	0.26	0.26	0.26	0.26	0.26	0.26	0.26	0.26	0.12	0.04	0.13
Quartz	0.20	0.20	0.20	0.20	0.20	0.20	0.20	0.20	0.22	0.29	0.14
Feldspar	0.03	0.03	0.03	0.03	0.03	0.03	0.03	0.03	0.15	0.16	0.13
Calcium smectite	0.11	0.12	0.13	0.14	0.10	0.11	0.11	0.11	0.15	0.16	0.16
Sodium smectite	0.11	0.12	0.13	0.14	0.11	0.11	0.11	0.11	0.14	0.14	0.15
Illite	0.26	0.26	0.26	0.26	0.24	0.28	0.30	0.32	0.05	0.06	0.09
Kaolinite	0.13	0.13	0.13	0.13	0.13	0.13	0.13	0.13	0.13	0.13	0.15

3.4.3 Initial Rock Conditions

Through the literature survey of the Da 'anzhai Member in the study area, it is found that the Da 'anzhai Member is mainly composed of three lithology: shell limestone, shale and argillaceous shell limestone. Three rock samples were measured by XRD, and the actual mineral content of the three lithologies in the study area was analyzed. According to the mineral content of the actual formation, the specific parameter settings of the one-dimensional and two-dimensional models are shown in Table 2.

There are nine rock mineral combinations in the one-dimensional model, corresponding to different mineral types and contents, as shown in Table 2. Case 1–12 selected R1, case 13–16 selected R1-R4, and the smectite content increased in turn. Case 17–20 selected R5-R8, and the illite content increased in turn.

In the two-dimensional model, the Da'anzhai member of the study area is mainly composed of three lithologies, which are R9 (mesoscopic tuff), R10 (shale), and R11 (muddy mesoscopic tuff), respectively. The mineral types and contents corresponding to the three lithologies are shown in Table 2.

3.4.4 Mineral kinetic parameters

The thermodynamic data of the minerals involved in the model were mostly taken from Wolery's EQ3/6 database (Wolery, 1992) while the kinetic data were taken from the TOUGHREACT database and related literature (Wolery, 1992; Xu et al., 2010), as detailed in Table 3.

4 Results

4.1 1D model

4.1.1 Clay mineral transformation

In this study, the results of all one-dimensional models have similarities in the whole trend. Taking Case 16 as an example, Figure 3 shows the relative mineral content variation curve after filling K-rich fluid between 0 and 2000 years. From Figures 3A, B, we can see the process of illitization, which can be described as decreasing smectite content and increasing illite content. Figure 3 shows that the mineral content changes greatly in the first 200 m, while after 200 m, the variation of mineral content is significantly weaker. On the time scale, the trend of mineral changes is obvious in the first 500 years of the reaction, with a rapid decrease from 8% to 5% in smectite content and a rapid increase from 1% to 24% in illite content, and this trend decreases when the reaction time is greater than 500 years.

The chemical equations involved above are as follows.

$$\text{Smectite} + Al^{3+} + K^{+} \rightarrow \text{Illite} + Na^{+} + Ca^{2+} + Fe^{3+} + Mg^{2+} + Si^{4+} \quad (1)$$

4.1.2 Different factors

Figure 4 demonstrates the variation of the mineral content of smectite illitization under different conditions in 2000 years Figure 4A indicates the variation of the relative content of illite under different

TABLE 3 Mineral kinetic parameters.

	Mineral species	A cm^2/g	Kinetic parameters							
			Medium mechanism		Acidic mechanism			Alkaline mechanism		
			K25 (mol/m_2 s) branch display	Ea (kJ/mol)	K25 (mol/m_2 s) branch display	Ea (kJ/mol)	n (H^+)	K25 (mol/m_2 s) branch display	Ea (kJ/mol)	n (H^+)
Minerals	Quartz	9.8	1.023e-14	87.7						
	Albite	9.8	2.574e-13	69.8	6.918e-11	65.0	0.457	2.512e-16	71.0	0.572
	Dolomite	9.8	2.951e-08	52.2	6.457e-04	36.1	0.5			
	K-feldspar	9.8	3.890e-13	38.0	8.710e-11	51.7	0.5	6.310e-22	94.1	−0.823
	Kaolinite	151.6	6.918e-14	22.2	4.898e-12	65.9	0.777	8.913e-18	17.9	0.472
	Smectite-Ca	151.6	1.660e-13	35.0	1.047e-11	23.6	0.34	3.020e-17	58.9	−0.40
	Smectite-Na	151.6	1.660e-13	35.0	1.041e-11	23.6	0.34	3.020e-17	58.9	−0.40
	Illite	151.6	1.660e-13	35.0	1.047e-11	23.6	0.34	3.020e-17	58.9	−0.40

Tips: A-Reaction specific surface area, unit: cm^2/kg; k25-Hydrodynamic constant at 25°C; Ea-Activation energy; n-Power ex.

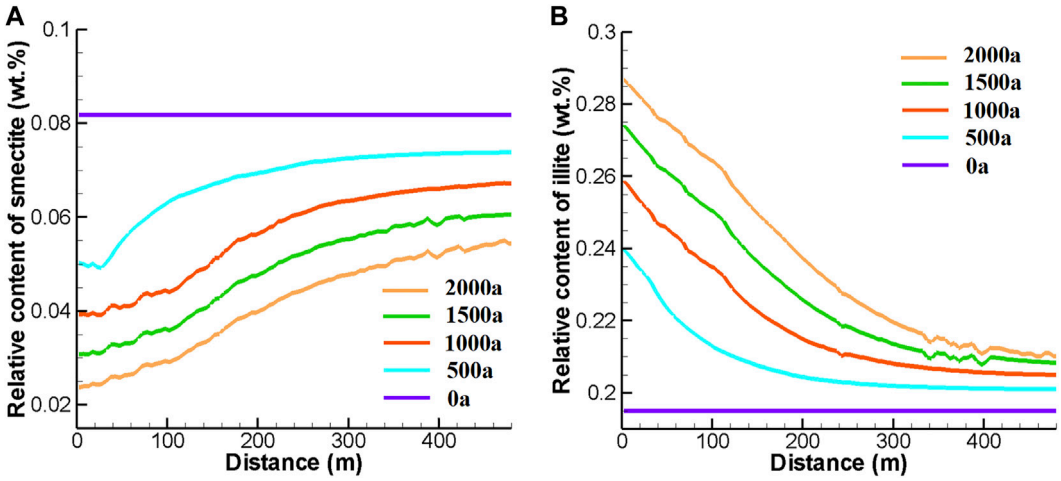

FIGURE 3
Variation of clay mineral transformation. (In the figure here and later, the "number + a" in the lower right corner represents the year).

temperature and pressure conditions in 2000 years. With the increase in temperature and pressure, the content of illite increases. When the temperature was below 110°C, the amount of illite conversion gradually increased as the temperature increased. By increasing the temperature from 50°C to 110°C, the conversion rate of smectite illitization increased by 275%. However, when the temperature was above 110°C, the amount of illite conversion gradually decreased as the temperature increased. When the temperature is over 115°C, or even 132°C, the degree of montmorillonite iliitization decreased. Therefore, 110°C–115°C is the optimum temperature for the conversion of clay minerals in the Da'anzhai member, Yuanba area.

Figures 4B, C show the variation of illite content under the conditions of different initial contents of illite and smectite. In the case of increasing the initial montmorillonite content, there is a promotion effect on the occurrence of montmorillonite illitization. Increasing the initial content of smectite from 0.22 to 0.28 increased the conversion of smectite illitization by 14.5%. However, increasing the illite content had almost no effect on the mineral transformation.

Figure 4D indicates the change of illite content under different K^+ concentration conditions. The diagram shows that the increase in K^+ concentration promotes the conversion of smectite to illite. When the K^+ concentration was lower than 1.0318×10^{-2} mol/L, the illite content in mineral transformation increased with the increase in K^+ concentration. When the K^+ concentration was higher than 1.0318×10^{-2} mol/L, the illite content in mineral transformation decreased gradually with the increase in K^+ concentration. Therefore, the K^+ concentration of 1.0318×10^{-2} mol/L is the optimum K^+ concentration for transforming of clay minerals in the Da'anzhai member, Yuanba area. Figure 4D shows that increasing the K^+ concentration from 3.4425×10^{-3} mol/L to 1.0318×10^{-2} mol/L resulted in a maximum increase in 20% in the conversion of smectite illitization.

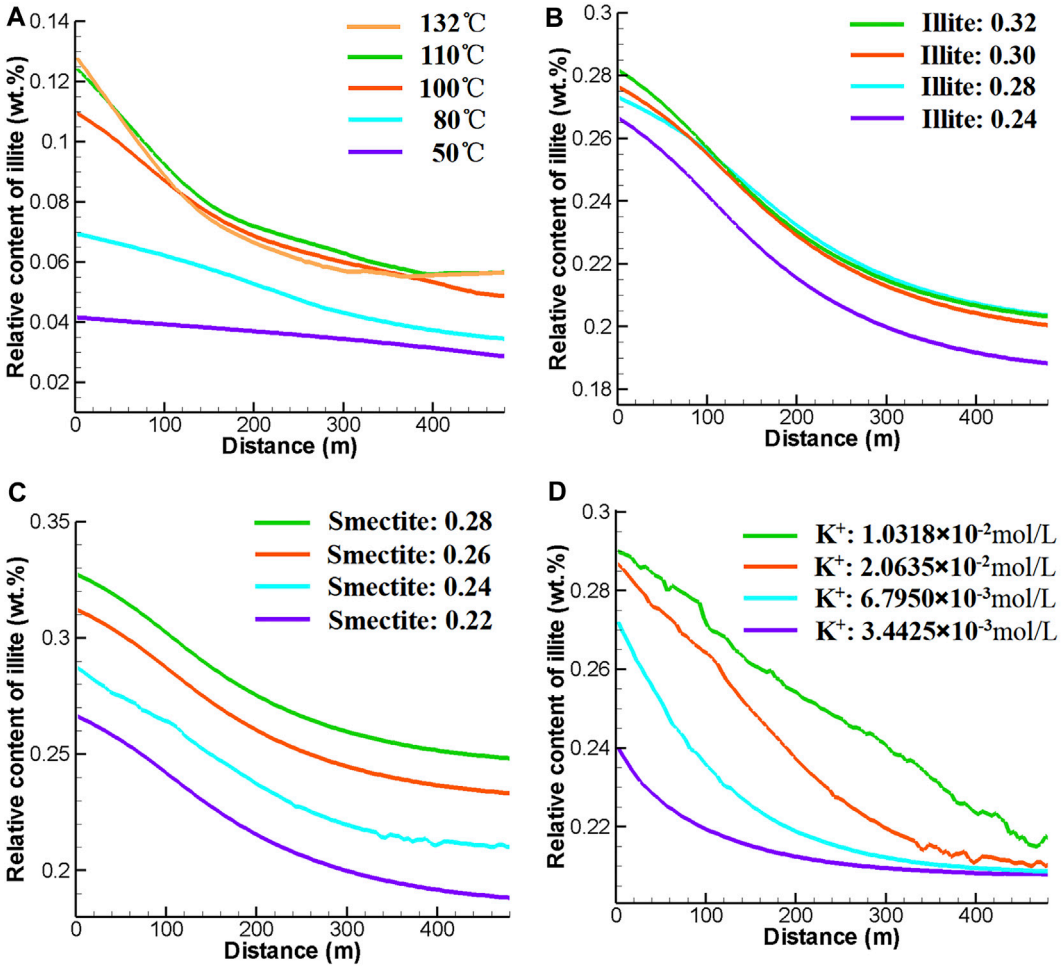

FIGURE 4
Variation of illite content under different conditions.

4.2 2-D model

4.2.1 Fluid migration

Figures 5A–F shows the migration of K-rich fluids in the formation after filling between 0 and 1,500 years. Overall, a dentate pattern gradually emerges as the fluid migration becomes more extensive, along with the continuous injection of K-rich fluid from the left side and spreads in all directions. This dentition became increasingly pronounced and finally distributed in a strip-like pattern at the edge. During the initial 10-year period, the injected fluid only migrated near the formation at the injection point, and the fluid pattern was micro-rectangular without dentation. The fluid continues to be injected. When the injected fluid migrated to 50 years, the fluid started to diffuse near the formation's top and bottom and reacted with the upper strata. The fluid also appears to have differential migration features, and the fluid pattern appears micro-dentation. When the fluid migration reached 500 years, the fluid migration difference further expanded, the dentation of the morphology became obvious, and the laminar structure of the dentate edge occurred. When the fluid diffusion reaches 1,500 years, the fluid migration distance is further expanded to about 500 m, and the final degree of fluid diffusion reaches about 40% of the total volume of the formation.

Figure 5 shows that the fluids show different migration characteristics in different strata, and the vertical heterogeneity is obvious. The physical properties of the muddy shale limestone, shale, and shale limestone decrease in turn, and the fluid preferentially enters into the muddy shale limestone layer with relatively good physical properties. When the fluid is migrated to 10 years, the fluid form of the muddy shale limestone layer appears convex; with the migration time, the convex form becomes more and more obvious; when the migration time reaches 1,500 years, the convex is most obvious, and the migration distance of the fluid of the muddy shale limestone layer differs from that of the shale layer fluid by 200 m.

4.2.2 Variation of different minerals

Figures 6J–L demonstrates the curves of the change in mineral content caused by K-rich fluids between 0 and 1,500 years. When the K-rich fluid is injected into the formation, the feldspar dissolves and releases K^+ in the acidic environment. The released K^+ and K^+ in the injected fluid promote smectite illitization.

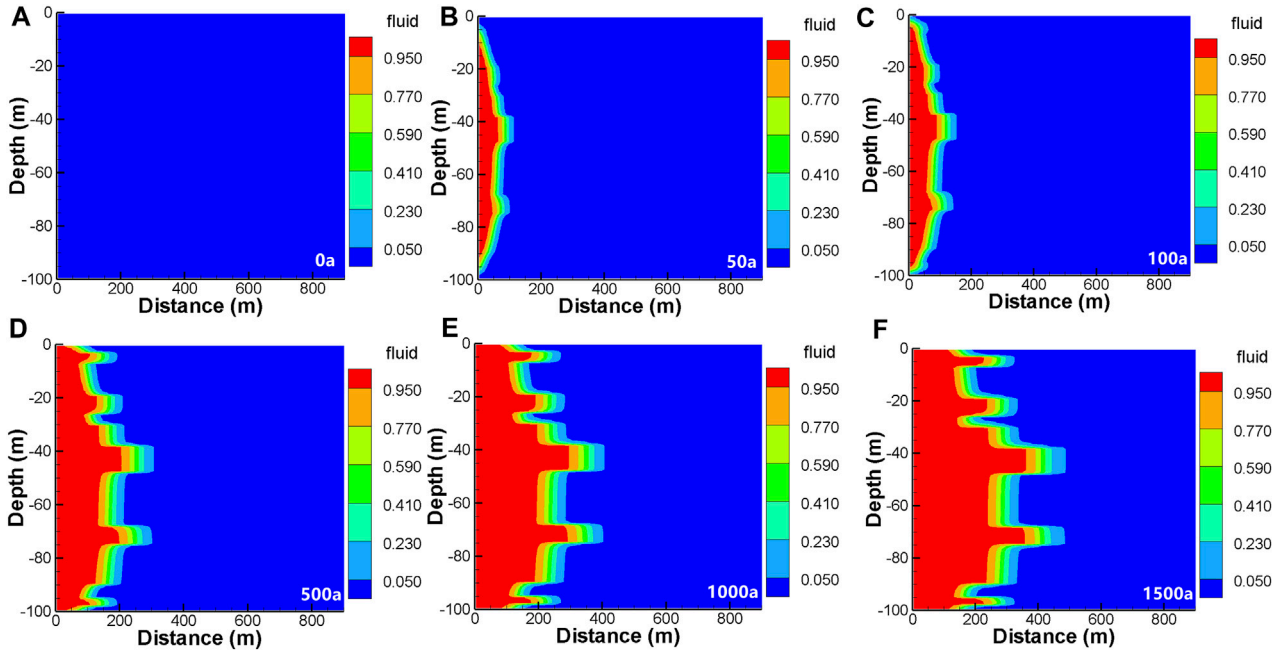

FIGURE 5
Fluid migration evolution diagram.

Figure 5 shows that between 0 and 1,500 years, the maximum distance of K-rich fluid migration is 500 m, and the fluid diffusion volume accounts for 40% of the total volume of the formation. Figures 6G–I indicates that between 0 and 1,500 years, smectite is consumed, and illite is generated at a distance of 200 m. Therefore, the smectite illitization rate in the Dazhai member is 40%.

Regarding the degree of reaction of the minerals, Figures 6A–F shows a difference in the degree of reaction between calcium montmorillonite and sodium montmorillonite. Comparing the graphs of the relative content changes of calcium montmorillonite and sodium montmorillonite under the same conditions (injection fluid, temperature, and pressure), the reaction time required for sodium montmorillonite is shorter (200–500 years shorter than that of calcium montmorillonite), and the illitization process is complete. Therefore, the conditions required for illite to occur in sodium smectite are lower than those required for calcium smectite, and sodium smectite is more prone to illitization.

The different physical properties of the three rock types in the Da'anzhai member, the existence of interstratigraphic heterogeneity, and the presence of K-rich fluids in the process of migration and participation in reactions lead to sequential differences in the process of feldspar dissolution, calcium smectite and sodium smectite consumption, and illite generation, that is, they show serrated structural in the change of minerals diagram.

The chemical equations involved above are as follows.

$$\text{Feldspar} + H_2O + H^+ \rightarrow (K^+, Na^+, Ca^{2+}) + Al^{3+} + H_4SiO_4\ (aq) \quad (2)$$

$$\text{Smectite} + Al^{3+} + K^+ \rightarrow \text{Illite} + Na^+ + Ca^{2+} + Fe^{3+} + Mg^{2+} + Si^{4+} \quad (3)$$

5 Discussion

5.1 Effect of temperature and pressure on the transformation of clay minerals

This study shows that temperature and pressure have important effects on mineral transformation. In this study, we simulated the effect on the conversion of smectite to illite at different burial depths, that is, different temperature and pressure conditions, respectively. It was found that the transformation of clay minerals was promoted with the increase in buried depth, namely, the increase in temperature and pressure.

The Ro value of vitrinite reflectance of Da'anzhai member in the Yuanba area is between 0.50% and 1.30%, and the organic matter is in the mature stage, during which the conversion of smectite to illite mainly occurs. The conversion of smectite to illite is mainly influenced by temperature, time and medium conditions, the temperature and pressure increase with the burial depth when the conversion of clay minerals occurs by precipitating interlayer water and cations (Renac and Meunier, 1995; Ferrage et al., 2011).

In the process of stratigraphic sedimentary evolution, the burial depth of sediments in the Da'anzhai member of Yuanba area is about 3,000 m in the A stage of middle diagenesis, the compaction is strong, and the rocks have been completely consolidated. At this stage, the diagenesis is mainly dominated by clay mineral transformation and accompanied by hydrocarbon generation evolution of organic matter. The vitrinite reflectance Ro value is between 0.50% and 1.30%. The organic matter evolution stage is in the thermocatalytic oil and gas generation stage, mainly generating oil and a small amount of wet gas, which is usually called the oil generation window (Liu and Zhang, 2007; Dziadzio and Matyasik,

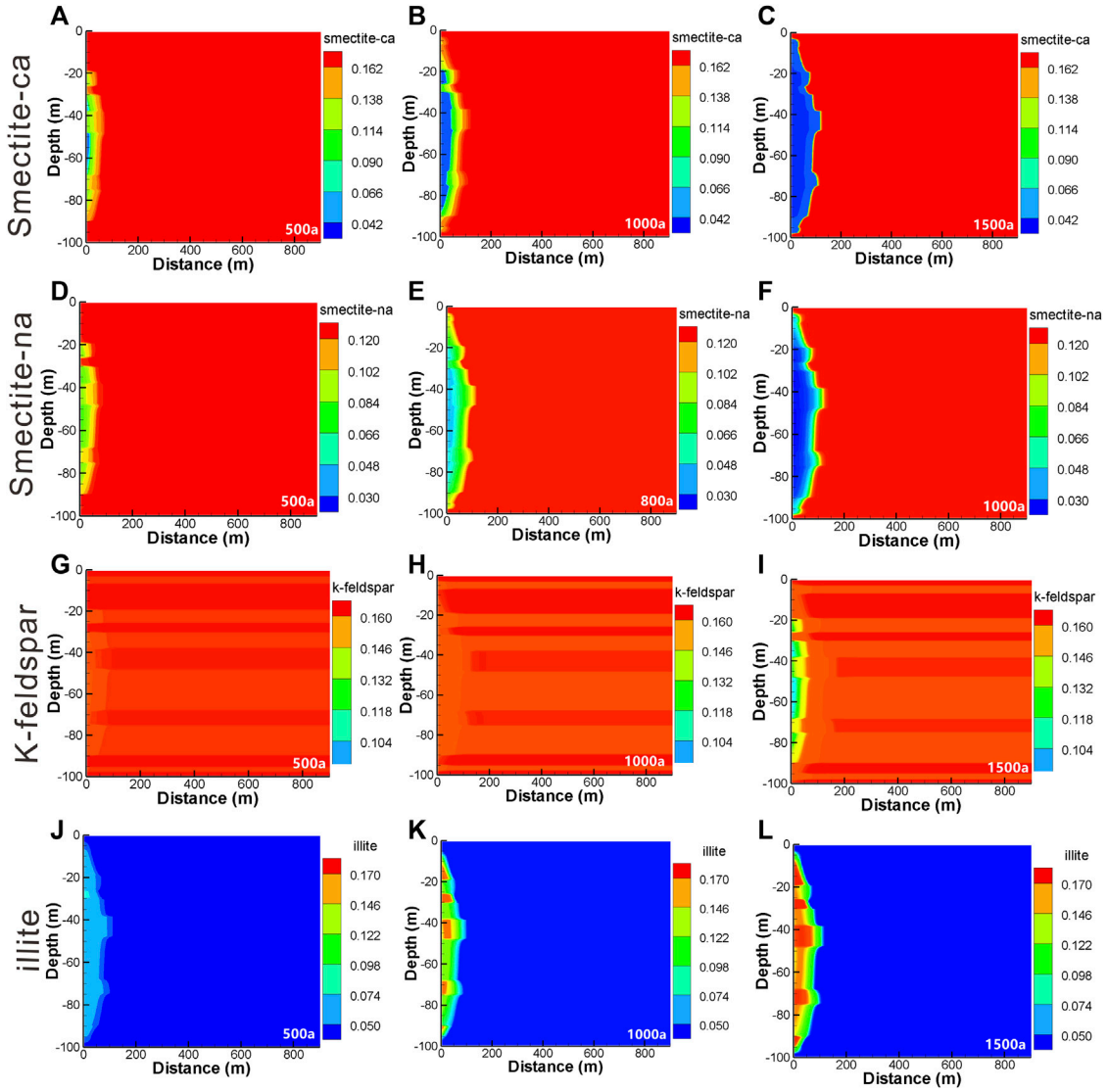

FIGURE 6
Variation of relative content of different minerals.

2021). During this stage, thermal degradation of the kerogen occurs, and the N, O, and S chemical bonds break to form acidic fluids such as CO_2, and H_2S, the development of organic acids provides conditions for the dissolution of K-feldspar in the formation (Welch and Ullman, 1996; Liu and Zhang, 2007; Yuan et al., 2019; Ma et al., 2022).

In this study, the conversion rate of smectite illitization increased as the temperature was increased from 50°C to 110°C. However, when the temperature was increased again to 132°C, the smectite illitization was inhibited instead. It can be inferred that the optimal temperature for K-feldspar dissolution to promote illitization is between 110°C and 132°C. Previous studies have shown that the evolution of mud shale diagenesis is divided into three ideal periods (Foscolos et al., 1976; Gong et al., 2021) These are syngenesis to early buried diagenesis, early buried diagenesis to paleogeotemperature of 120°C–140°C, and paleogeotemperature greater than 120°C–140°C (Foscolos et al., 1976; Zhou et al., 2012; Chen et al., 2016; Gong et al., 2021). During the first period, early diagenesis, K-feldspar was not preferentially dissolved due to the low temperatures, and the reaction was blocked and did not provide significant amounts of K^+ (Wilkimson et al., 2001; Zhou et al., 2012). And in the initial stage of buried diagenesis 120°C–140°C, almost all dissolution of preserved K-feldspar occurs to form kaolinite and K^+, accompanied by the conversion of smectite to illite, and secondary pores can be dissolved by stable K-feldspar or unstable acidic feldspar. However, in the late diagenesis, when the paleogeotherm is greater than 120°C–140°C, the formation is closed and appears to be kaolinite illitization (Higgs et al., 2007).

In the Da'anzhai member, Yuanba area, during the conversion of smectite to illite, part of the K^+ originates from the dissolution of K-feldspar by underground acidic

fluids (Welch and Ullman, 1996; Yuan et al., 2019; Ma et al., 2022). With the increase in buried depth and ground temperature, the dissolution of K-feldspar by the underground acidic fluid is enhanced; when the ground temperature is less than 110°C, the conversion of smectite and kaolinite to illite is enhanced with the increase in ground temperature, when the ground temperature reaches 110°C–115°C, the dissolution of K-feldspar by the acidic fluid is stable. In summary, for the Da'anzhai member in the Yuanba area, the upper limit temperature for the conversion of smectite and kaolinite to illite is 110°C–115°C. For the Da'anzhai Member in Yuanba area of Sichuan Basin, temperature and pressure do not directly affect the transformation of smectite to illite but indirectly influence the K^+ required, which affects the mineral conversion.

Appropriate pressure is also a prerequisite for clay mineral transformation (Kamp, 2008; Duan et al., 2018). The dissolution of K-feldspar in the early stage provides large amounts of K^+, and large amounts of illite precipitation are produced under K-rich fluids. At the same time, mineral dissolution leads to the destruction of loaded particles in the fine-grained rocks, the interparticle support force within the fine-grained rocks decreases, and the overlying formation pressure is transferred to the pore fluid, resulting in overpressure. Overpressure inhibits clay mineral transformations (Duan et al., 2018). Therefore, during the transformation of clay minerals in the overpressure zone, the discharge of H^+, interlayer water and various cations from the mudstone will be slowed down (Duan et al., 2018).

5.2 The influence of different minerals on the transformation of clay minerals

In this study, the increase of the initial content of smectite promoted the transformation of minerals. Figure 4C shows that the initial smectite content increases from 0.22 to 0.28, and the content of illite increases from 0.265 to 0.328. It can be seen that the initial content of smectite will affect its transformation and promote mineral transformation. Figure 4B shows that the initial content of illite has little effect on the transformation of minerals.

In essence, the conversion of smectite to illite is not a simple chemical reaction but a complex physical and chemical reaction (physicochemical reaction). That is, in the compaction diagenesis, with the increase in burial depth, formation temperature, and formation pressure, smectite among the interlayer water, and pore water. Adsorbed water continues to precipitate, and the smectite lattice of Na^+, Ca^{2+}, Fe^{2+} and Mg^{2+} are separated, leading to lattice rearrangement, and then the process of K^+, H^+ being inserted into the lattice, participating in the reaction and finally transforming into illite (Oueslati, 2019; Li et al., 2021).

The dissolution of feldspar-like minerals produces kaolinite and siliceous, 20%–30% of the mass of smectite will be converted to siliceous, resulting in increasing brittle minerals, which are prone to structural fractures under tectonic stress (Ruiz Cruz and Reyes, 1998; Li et al., 2020b). As an effective supporting mineral in shale matrix, brittle minerals have high mechanical properties of brittle rocks with high compressive strength, high elastic modulus and low Poisson's ratio, they play an anti-compaction role in the process of multi-stage geological tectonic movement so that the intergranular pores around mineral particles and the intragranular pores inside mineral particles are relatively effectively protected, and most of the intergranular pores and intragranular pores around mineral particles belong to macropores. The brittle minerals have a certain protective effect on the reservoir (Wang et al., 2016; Yasin et al., 2017; Wang et al., 2022).

Clay minerals often contain pore water, adsorbed water, interlayer water and structural water, the dehydration and transformation of clay minerals is a powerful mechanism for fracture development in tight shale, which is the main occurrence space of shale gas (Villabona-Estupiñán et al., 2017). From the transformation mechanism of smectite to illite, this transformation is a solid-phase transformation (Olives et al., 2000; Chen et al., 2004; Ji et al., 2018).

In the sandstone reservoirs of the first member of paleogene Shahejie Formation in the Zhengjia-Wangzhuang area of the Dongying Sag, when the content of smectite layer in S/I is equal, the expansion rate and cation exchange values of the sodium type S/I are large, the calcium type value is small, and the calcium-sodium transition type value is medial (Zhang et al., 2004). In fact, the process of clay mineral transformation and expansion is actually a cation exchange process, the difference in the mechanism of water expansion between calcium smectite and sodium smectite results in the difference in illitization, the calcium smectite layers only undergo lattice expansion when exposed to water, while sodium smectite layers not only undergo lattice expansion but also undergo osmotic hydration expansion, and the volume after osmotic hydration expansion is about 20 times after lattice expansion (Teppen and Miller, 2006; Shao et al., 2010; Ruan et al., 2022). Another reason for this phenomenon is that smectite illitization is a kind of ion recombination in the interlayer domain of 2:1 type clay mineral, so the sodium ion bonds are more likely to break, so K^+ enter into the lattice of sodium smectite more easily and occurs illitization. Therefore, in the Da'anzhai Member, smectite is more likely to undergo illitization during the process of sodium smectite illitization.

5.3 Effect of fluids on clay mineral transformation

The Da'anzhai member reservoir is in the lentic environment, and the formation of minerals is closely related to fluid action, overall, the fluids that strongly impact on the Da'anzhai Member include several types, such as K-rich fluids, CO_2 and organic acids (He et al., 2022). From this one-dimensional mechanism model, it can be found that the increase in K^+ in the fluid promotes the transformation of smectite to illite. When the K^+ concentration is lower than 1.0318×10^{-2} mol/L, it has a great influence on the transformation of minerals; however, when the K^+ concentration is higher than 1.0318×10^{-2} mol/L, the promoting effect on the transformation of minerals becomes weaker.

It has been suggested that the generation of dissolution pores is related to organic acid filling in the Da'anzhai member, where acidic fluid filling leads to the dissolution of minerals and the release of large amounts of alkaline ions. It can produce alkaline supersaturated fluids and provide a material basis for the generation of carbonate cement (Xu et al., 2010; Ferrage et al.,

2011). Late organic acid filling increases the acidity of the solution, resulting in early calcite cement dissolution and the dissolution of feldspar and other minerals. Feldspar dissolution generates clay minerals dominated by kaolinite, and releases silica to form quartz secondary enlargement edge (Ruiz Cruz and Reyes, 1998; Li et al., 2020a). With the further increase in burial depth, the increase in formation temperature and formation pressure, kaolinite, smectite and other clay minerals react with K^+ generated by dissolution of feldspathic minerals, thus further transforming into illite and illite-montmorillonite mixed layer and forming pores between clay minerals, eventually leading to the main types of clay minerals in this area are illite, illite-montmorillonite mixed layer and smectite. At the same time, the organic acid and CO_2 filling provided the material basis for the precipitation of carbonate minerals, leading to late carbonate cement forming.

6 Conclusion

The conversion of smectite to illite in the Da 'anzhai Member is a complex physical and chemical process, which is affected by many factors such as temperature, pressure, fluid, organic acid and lithology. Firstly, the increase of temperature can promote illitetion, but the critical temperature is about 100°C–115°C. Below the critical temperature, the conversion efficiency of smectite to illite increases with the increase of temperature. However, when the temperature is higher than the critical temperature, the illite effect decreases with the increase of temperature. In addition, the concentration of K^+ also affects the conversion of smectite to illite, and the boundary concentration of K^+ is about 1.0318×10^{-2} mol/L. When the concentration is lower than the critical concentration, with the increase of K^+ concentration, the illite effect is enhanced. When the concentration of illite is higher than the critical concentration, with the increase of K^+ concentration, the illitization is weakened. Finally, the appropriate pressure and organic acid have an important influence on the illite in the Da 'anzhai Member. The acidic fluid promotes the dissolution of K-feldspar and releases K^+ to provide a material basis for the illite of smectite.

Data availability statement

The original contributions presented in the study are included in the article/Supplementary material, further inquiries can be directed to the corresponding author.

Author contributions

Conceptualization, LY and LL; methodology, LY and XL; software, LY and XL; validation, JH; formal analysis, LY and YS; investigation, XL and WL; resources, LL; data curation, LY and WL; writing—original draft preparation, LY, LL, and MS; writing—review and editing, CM, JH, BL and JX. All authors contributed to the article and approved the submitted version.

Funding

This research are supported by the SINOPEC Key Laboratory of Petroleum Accumulation Mechanisms (33550007-21-ZC0613-0061), China Geological Survey Second-level Project (No.DD20230025) and Development project of Xinjiang conglomerate reservoir Laboratory (Grant No. 2020D04045).

Acknowledgments

We are sincerely grateful to the handling editor and reviewers who provided valuable comments. The authors also sincerely appreciate the support from the SINOPEC Key Laboratory of Petroleum Accumulation Mechanisms (33550007-21-ZC0613-0061).

Conflict of interest

LY, LL, and JX are employed by SINOPEC Key Laboratory of Petroleum Accumulation Mechanisms. MS was employed by Exploration and Development Research Institute of Huabei Oilfield Company, China National Petroleum Corporation. BL was employed by Xinjiang Oilfield Company.

The remaining authors declare that the research was conducted in the absence of any commercial or financial relationships that could be construed as a potential conflict of interest.

The authors declare that this study received funding from SINOPEC Key Laboratory of Petroleum Accumulation Mechanisms (33550007-21-ZC0613-0061), China Geological Survey Second-level Project (No. DD20230025) and Development project of Xinjiang conglomerate reservoir Laboratory (Grant No. 2020D04045). The funder had the following involvement in the study: design and the decision to submit it for publication.

Publisher's note

References

Baruch, E. T., Kennedy, M. J., Löhr, S. C., and Dewhurst, D. N. (2015). Feldspar dissolution-enhanced porosity in paleoproterozoic shale reservoir facies from the barney creek formation (McArthur basin, Australia). *Bulletin* 99, 1745–1770. doi:10.1306/04061514181

Bernard, S., Wirth, R., Schreiber, A., Schulz, H.-M., and Horsfield, B. (2012). Formation of nanoporous pyrobitumen residues during maturation of the barnett shale (fort worth basin). *Int. J. Coal Geol.* 103, 3–11. doi:10.1016/j.coal.2012.04.010

Bjlykke, K. (1998). Clay mineral diagenesis in sedimentary basins — a key to the prediction of rock properties. Examples from the north sea basin. *Clay Miner.* 33, 15–34. doi:10.1180/000985598545390

Borjigin, T., Lu, L., Yu, L., Zhang, W., Pan, A., Shen, B., et al. (2021). Formation, preservation and connectivity control of organic pores in shale. *Petroleum Explor. Dev.* 48, 798–812. doi:10.1016/S1876-3804(21)60067-8

Chen, S., Han, Y., Fu, C., Zhang, h., Zhu, Y., and Zuo, Z. (2016). Micro and nano-size pores of clay minerals in shale reservoirs: implication for the accumulation of shale gas. *Sediment. Geol.* 342, 180–190. doi:10.1016/j.sedgeo.2016.06.022

Chen, T., Xu, H., Lu, A., Xu, X., Peng, S., and Yue, S. (2004). Direct evidence of transformation from smectite to palygorskite: TEM investigation. *D-Earth Sci.* 47, 985–994. doi:10.1360/03yd0509

Duan, W., Li, C.-F., Luo, C., Chen, X.-G., and Bao, X. (2018). Effect of formation overpressure on the reservoir diagenesis and its petroleum geological significance for the DF11 block of the Yinggehai Basin, the South China Sea. *Mar. Petroleum Geol.* 97, 49–65. doi:10.1016/j.marpetgeo.2018.06.033

Dziadzio, P. S., and Matyasik, I. (2021). Sedimentological and geochemical characterisation of the lower oligocene menilite shales from the magura, dukla, and silesian nappes, polish outer carpathians - a new concept. *Mar. Petroleum Geol.* 132, 105247. doi:10.1016/j.marpetgeo.2021.105247

Ferrage, E., Vidal, O., Mosser-Ruck, R., Cathelineau, M., and Cuadros, J. (2011). A reinvestigation of smectite illitization in experimental hydrothermal conditions: results from X-ray diffraction and transmission electron microscopy. *Am. Mineralogist* 96, 207–223. doi:10.2138/am.2011.3587

Foscolos, A. E., Powell, T. G., and Gunther, P. R. (1976). The use of clay minerals and inorganic and organic geochemical indicators for evaluating the degree of diagenesis and oil generating potential of shales. *Geochimica Cosmochimica Acta* 40, 953–966. doi:10.1016/0016-7037(76)90144-7

Gong, L., Wang, J., Gao, S., Fu, X., Liu, B., Miao, F., et al. (2021). Characterization, controlling factors and evolution of fracture effectiveness in shale oil reservoirs. *J. Petroleum Sci. Eng.* 203, 108655. doi:10.1016/j.petrol.2021.108655

Gracceva, F., and Zeniewski, P. (2013). Exploring the uncertainty around potential shale gas development – a global energy system analysis based on TIAM (TIMES Integrated Assessment Model). *Energy* 57, 443–457. doi:10.1016/j.energy.2013.06.006

He, W., Bai, X., Meng, Q., Li, J., Zhang, D., and Gotoh, Y. (2022). Accumulation geological characteristics and major discoveries of lacustrine shale oil in Sichuan Basin. *Acta Pet. Sin.* 43, 885–898. doi:10.7623/syxb2022.07.001

Higgs, K., Horst, Z., Reyes, A., and Funnell, R. (2007). Diagenesis, porosity evolution, and petroleum emplacement in tight gas reservoirs, taranaki basin, New Zealand. *J. Sediment. Res.* 77 (12), 1003–1025. doi:10.2110/jsr.2007.095

Ji, S., Zhu, J., H, H., Tao, Q., Zhu, R., Ma, L., et al. (2018). Conversion of serpentine to smectite under hydrothermal condition: implication for solid-state transformation. *Am. Mineralogist* 103 (2), 241–251. doi:10.2138/am-2018-6183CCBYNCND

Jiang, D., Li, P., Zheng, M., Chen, Q., Xiong, W., and Zou, H. (2023a). Impacts of different matrix components on multi-scale pore structure and reservoir capacity: insights from the Jurassic Da'anzhai member in the Yuanba area, Sichuan Basin. *Energy Rep.* 9, 1251–1264. doi:10.1016/j.egyr.2022.12.020

Jiang, T., Jin, Z., Qiu, H., Chen, X., Zhang, Y., and Su, Z. (2023b). Pore structure and gas content characteristics of lower jurassic continental shale reservoirs in northeast sichuan, China. *China. Nanomater.* 13, 779. doi:10.3390/nano13040779

Jiao, F., Zou, C., and Yang, Z. (2020). Geological theory and exploration & development practice of hydrocarbon accumulation inside continental source kitchens. *Petroleum Explor. Dev.* 47, 1147–1159. doi:10.1016/S1876-3804(20)60125-8

Kamiński, M., Muthuraman, M., Łagocka, A., and Cholewiński, M. (2017). Shale gas as a pro-environmental source of energy. *Ciepłownictwo, Ogrzew. Went.* 48 (4), 141. doi:10.15199/9.2017.4.2IF

Kamp, P. (2008). Smectite-illite-muscovite transformations, quartz dissolution, and silica release in shales. *Clays Clay Minerals* 56 (1), 66–81. doi:10.1346/CCMN.2008.0560106

Kang, J., Wang, Z., Xie, S., Zeng, D., Du, Y., Z, R., et al. (2022). Lithofacies types and reservoir characteristics of shales of Jurassic Da'anzhai member in central Sichuan Basin. *Lithol. Reserv.* 34 (4), 53–65. doi:10.12108/yxyqc.20220406

Li, C., Liu, D., Xiao, L., Jiang, Z., Li, Z., and Guo, J. (2021). Research into pore evolution in Cretaceous continental shales in the Songliao Basin. *Petroleum Sci. Bull.* 6, 181–195. doi:10.3969/j.issn.2096-1693.2021.02.015

Li, L., Li, P., Zhang, Z., Hao, J., Xiao, J., and Zou, H. (2020a). Quantitative characterization of microscopic pore structure of shale in Da'anzhai member in Yuanba area, northern Sichuan Basin. *Sci. Technol. Eng.* 20, 8923–8932. doi:10.3969/j.issn.1671-1815.2020.22.011

Li, Y., Xu, W., Wu, P., and Meng, S. (2020b). Dissolution versus cementation and its role in determining tight sandstone quality: a case study from the upper paleozoic in northeastern ordos basin, China. *J. Nat. Gas Sci. Eng.* 78, 103324. doi:10.1016/j.jngse.2020.103324

Liu, G. (2021). Challenges and countermeasures of log evaluation in unconventional petroleum exploration and development. *Petroleum Explor. Dev.* 48, 1033–1047. doi:10.1016/S1876-3804(21)60089-7

Liu, W., and Zhang, D. (2007). Deep-seated gas generation and preservation condition in China. *Earth Sci. China* 1, 351–357. doi:10.1007/s11707-007-0043-0

Liu, Z., Liu, G., Hu, Z., Feng, D., Zhu, T., Bian, R., et al. (2020). Lithofacies types and assemblage features of continental shale strata and their implications for shale gas exploration: a case study of the middle and lower jurassic strata in the Sichuan Basin. *Nat. Gas. Ind. B* 7, 358–369. doi:10.1016/j.ngib.2019.12.004

Liu, Z., Qiu, H., Jiang, Z., Liu, R., Wei, X., Chen, F., et al. (2021). Types and quantitative characterization of microfractures in the continental shale of the da'anzhai member of the Ziliujing Formation in northeast sichuan, China. *China. Miner.* 11, 870. doi:10.3390/min11080870

Ma, L., Taylor, K. G., Dowey, P. J., Courtois, L., Gholinia, A., and Lee, P. D. (2017). Multi-scale 3D characterisation of porosity and organic matter in shales with variable TOC content and thermal maturity: examples from the Lublin and Baltic Basins, Poland and Lithuania. *Int. J. Coal Geol.* 180, 100–112. doi:10.1016/j.coal.2017.08.002

Ma, Z., Tan, J., Zheng, L., Ni, C., Hu, R., and Ma, J. (2022). Simulation experiment of fluid-feldspar sandstone interactions and their implications for tight oil and gas exploration of the Yanchang Formation, Ordos Basin, China. *Mar. Petroleum Geol.* 142, 105737. doi:10.1016/j.marpetgeo.2022.105737

Olives, J., Amouric, M., and Perbost, R. (2000). Mixed layering of illite-smectite: results from high-resolution transmission electron microscopy and lattice-energy calculations. *Clays Clay Minerals* 48 (2), 282–289. doi:10.1346/CCMN.2000.0480215

Oueslati, W. (2019). Effect of soil solution pH during the tetracycline intercalation on the structural properties of a dioctahedral smectite: microstructural analysis. *J. Nanomater.* 2019, 1–17. doi:10.1155/2019/7414039

Renac, C., and Meunier, A. (1995). Reconstruction of palaeothermal conditions in a passive margin using illite-smectite mixed-layer series (Ba1 scientific deep drill-hole, ardeche, France). *Clay Miner.* 30, 107–118. doi:10.1180/claymin.1995.030.2.03

Ruan, K., Komine, H., Wang, H., Ito, D., and Gotoh, T. (2022). Experimental study on swelling pressure of low dry density compacted bentonites during saturation combining X-ray diffraction. *Can. Geotechnical J.* 60 (4), 566–579. doi:10.1139/cgj-2020-0342

Ruiz Cruz, M. D., and Reyes, E. (1998). Kaolinite and dickite formation during shale diagenesis: isotopic data. *Appl. Geochem.* 13, 95–104. doi:10.1016/S0883-2927(97)00056-5

Sca, B., Jlb, C., Clb, D., Jy, E., Yong, L. B., Sl, E., et al. (2019). Factors controlling the reservoir accumulation of triassic chang 6 member in jiyuan-wuqi area, ordos basin, NW China. *Petroleum Explor. Dev.* 46, 253–264. doi:10.1016/S1876-3804(19)60006-6

Shangbin, C., Yanming, Z., Si, C., Yufu, H., Changqing, F., and Junhua, F. (2017). Hydrocarbon generation and shale gas accumulation in the longmaxi formation, southern Sichuan Basin, China. *Mar. Petroleum Geol.* 86, 248–258. doi:10.1016/j.marpetgeo.2017.05.017

Shao, H., Ray, J., and Jun, Y-S. (2010). Dissolution and precipitation of clay minerals under geologic CO2 sequestration conditions: CO2–Brine–Phlogopite interactions. *Environ. Sci. Technol.* 44 (15), 5999–6005. doi:10.1021/es1010169

Shuen, A., Feiler, P. F., and Teece, D. J. (2014). Dynamic capabilities in the upstream oil and gas sector: managing next generation competition. *Energy Strategy Rev.* 3, 5–13. doi:10.1016/j.esr.2014.05.002

Sun, J., Tian, Z., Shen, Y., Liu, B., Xu, Q., and Wang, Y. (2020). Differential diagenetic evolution and hydrocarbon charging of the tight limestone reservoir of the Da'anzhai Member in the central Sichuan Basin, China. *Interpretation* 8 (4), T1007–T1022. doi:10.1190/INT-2018-0192.1

Tan, M., Liu, Z., Shen, F., Xie, R., Liu, C., Deng, K., et al. (2016). Features and model of mixed sediments of Da'anzhai member in lower jurassic Ziliujing Formation,huilong area,Sichuan Basin. *Acta Sedimentol. Sin.* 34 (3), 571–581. doi:10.14027/j.cnki.cjxb.2016.03.015

Teppen, B. J., and Miller, D. M. (2006). Hydration energy determines isovalent cation exchange selectivity by clay minerals. *Soil Sci. Soc. Am. J.* 70, 31–40. doi:10.2136/sssaj2004.0212

Villabona-Estupiñán, S., de Almeida Rodrigues, J., and Nascimento, R. (2017). Understanding the clay-PEG (and hydrophobic derivatives) interactions and their effect on clay hydration and dispersion: a comparative study. *Appl. Clay Sci.* 143, 89–100. doi:10.1016/j.clay.2017.03.021

Wang, R., Ding, W., Zhang, Y., Wang, Z., Wang, X., He, J., et al. (2016). Analysis of developmental characteristics and dominant factors of fractures in lower cambrian marine shale reservoirs: a case study of niutitang Formation in cen'gong block, southern China. *J. Petroleum Sci. Eng.* 138, 31–49. doi:10.1016/j.petrol.2015.12.004

Wang, S., Wu, Z., Chen, J., Liu, H., Wang, R., and Liu, J. (2022). Study of the effect of mineral components on the permeability impairment rate and stress sensitivity factor of shale. *Geofluids* 2022, 1–15. doi:10.1155/2022/4407252

Welch, S. A., and Ullman, W. J. (1996). Feldspar dissolution in acidic and organic solutions: compositional and pH dependence of dissolution rate. *Geochimica Cosmochimica Acta* 60, 2939–2948. doi:10.1016/0016-7037(96)00134-2

Wilkinson, M., Milliken, K., and Haszeldine, R. (2001). Systematic destruction of K-feldspar in deeply buried rift and passive margin sandstones. *J. Geol. Soc.* 158 (4), 675–683. doi:10.1144/jgs.158.4.675

Wolery, T J. (1992). *EQ3/6, a software package for geochemical modeling of aqueous systems: Package overview and installation guide (Version 7.0)*. United States: Office of Scientific & Technical Information Technical Reports. doi:10.2172/2F138894

Xie, R., Zhang, S., Zhou, L., Liu, H., Y, M., and J, X. (2023). Hydrocarbon accumulation characteristics of tight reservoirs of Da'anzhai member of Jurassic Ziliujing Formation in eastern Sichuan Basin. *Lithol. Reserv.* 35 (1), 108–119. doi:10.12108/yxyqc.20230110

Xiong, S., Gao, Z., Wei, W., and Wang, Y. (2023). Differential effects of pore structure of mineral and maceral components on the methane adsorption capacity evolution of the lower jurassic Da'anzhai member of the Ziliujing Formation lacustrine shale, Sichuan Basin, China. *Mar. Petroleum Geol.* 147, 106017. doi:10.1016/j.marpetgeo.2022.106017

Xu, Q., Liu, B., Song, X., Wang, Q., Chen, X., Li, Y., et al. (2022). Hydrocarbon generation and organic matter enrichment of limestone in a lacustrine mixed sedimentary environment: a case study of the jurassic Da'anzhai member in the central Sichuan Basin, SW China. *Petroleum Sci.* 20, 670–688. doi:10.1016/j.petsci.2022.10.002

Xu, Q., Ma, Y., Liu, B., Song, X., Su, J., and Chen, Z. (2019). Characteristics and control mechanism of nanoscale pores in lacustrine tight carbonates: examples from the Jurassic Da'anzhai Member in the central Sichuan Basin, China. *J. Asian Earth Sci.* 178, 156–172. doi:10.1016/j.jseaes.2018.05.009

Xu, T., Kharaka, Y. K., Doughty, C., Freifeld, B. M., and Daley, T. M. (2010). Reactive transport modeling to study changes in water chemistry induced by CO_2 injection at the Frio-I Brine Pilot. *Chem. Geol.* 271, 153–164. doi:10.1016/j.chemgeo.2010.01.006

Xu, T., Sonnenthal, E., Spycher, N., and Pruess, K. (2006). TOUGHREACT—a simulation program for non-isothermal multiphase reactive geochemical transport in variably saturated geologic media: applications to geothermal injectivity and CO_2 geological sequestration. *Comput. Geosciences* 32, 145–165. doi:10.1016/j.cageo.2005.06.014

Yang, L., Li, X., Wei, G., Liu, Y., Zhuo, Q., Yu, Z., et al. (2023). Effects of deep alkaline and acidic fluids on reservoir developed in fault belt of saline lacustrine Basin. *Pet. Sci.* 2 (20), 776–786. doi:10.1016/j.petsci.2022.09.020

Yang, R., Wang, F., Yun, N., Zeng, H., Han, Y., Hu, X., et al. (2022). Pore structure characteristics and permeability stress sensitivity of jurassic continental shale of dongyuemiao member of Ziliujing Formation, fuxing area, eastern Sichuan Basin. *Minerals* 12, 1492. doi:10.3390/min12121492

Yang, X., Chen, C., and Wang, X. (2020). Sedimentary facies analysis of lacustrine carbonate in the Da'anzhai member, Ziliujing Formation, lower jurassic, in northeastern Sichuan Basin. *ResearchGate* 2020, 4. doi:10.16509/j.georeview

Yasin, Q., Du, Q., Sohail, G. M., and Ismail, A. (2017). Impact of organic contents and brittleness indices to differentiate the brittle-ductile transitional zone in shale gas reservoir. *Geosci. J.* 21, 779–789. doi:10.1007/s12303-017-0007-7

Yuan, G., Cao, Y., Schulz, H.-M., Hao, F., Gluyas, J., Liu, K., et al. (2019). A review of feldspar alteration and its geological significance in sedimentary basins: from shallow aquifers to deep hydrocarbon reservoirs. *Earth-Science Rev.* 191, 114–140. doi:10.1016/j.earscirev.2019.02.004

Zhang, D., Zhou, C. H., Lin, C. X., Tong, D. S., and Yu, W. H. (2010). Synthesis of clay minerals. *Appl. Clay Sci.* 50, 1–11. doi:10.1016/j.clay.2010.06.019

Zheng, R., He, L., Liang, X., and Xu, W. (2013). Forming conditions of shale gas (oil) plays in the Lower Jurassic Da′anzhai member in the eastern Sichuan Basin. *Nat. Gas. Ind.* 33 (12), 30–40. doi:10.3787/j.issn.1000-0976.2013.12.004

Zhou, H., Huang, S., and Lan, Y. (2012). Types of clay minerals and its effects on reservoir properties of Chang 6 oil reservoir set in Huaqing area,Ordos Basin. *Lithol. Reserv.* 24, 66–73. doi:10.3969/j.issn.1673-8926.2012.03.013

Zhu, Y., Li, Z., Zeng, L., Liu, Z., and Wang, X. (2022). Diagenesis and its impact on the reservoir quality of continental shales: a case study of the lower jurassic Da'anzhai member of the Ziliujing Formation in the Sichuan Basin, China. *Geofluids* 2022, 1–21. doi:10.1155/2022/5942370

Zou, C., Qiu, Z., Zhang, J., Li, Z., Wei, H., Liu, B., et al. (2022). Unconventional petroleum sedimentology: a key to understanding unconventional hydrocarbon accumulation. *Engineering* 18, 62–78. doi:10.1016/j.eng.2022.06.016

Zou, C., Yang, Z., Sun, S., Zhao, Q., Bai, W., Liu, H., et al. (2020). Exploring petroleum inside source kitchen": shale oil and gas in Sichuan Basin. *Sci. China Earth Sci.* 63, 934–953. doi:10.1007/s11430-019-9591-5